

# Chronic Ingestion of Ethanol Induces Hepatocellular Carcinoma in Mice Without Additional Hepatic Insult

Mutsumi Tsuchishima · Joseph George ·  
Hisakazu Shiroeda · Tomiyasu Arisawa ·  
Tsutomu Takegami · Mikihiro Tsutsumi

Received: 17 October 2012 / Accepted: 11 January 2013 / Published online: 31 January 2013  
© Springer Science+Business Media New York 2013

## Abstract

**Background** Chronic intake of alcohol increases the risk of gastrointestinal and hepatic carcinogenesis. The present study was focused to investigate the incidence and mechanism of pathogenesis of hepatocellular carcinoma (HCC) during chronic ingestion of alcohol without any additional hepatic injury.

**Methods** Ethanol was administered to Institute for Cancer Research male mice through drinking water for 70 weeks at concentrations of 5 % (first week), 10 % (next 8 weeks), and 15 % thereafter. The animals were killed at 60 and 70 weeks, the livers were examined for hepatic tumors, and evaluated for foci of cellular alteration (FCA). Immunohistochemical staining was performed in the liver sections for cytochrome P4502E1 (CYP2E1), 4-hydroxy-nonenal (4-HNE), and proto-oncogene, c-Myc.

**Results** At the 60th week, 40 % of the mice in the ethanol group had visible white nodules (5–10 mm) in the liver, but not in the control mice. At the 70th week, several larger nodules (5–22 mm) were present in the livers of 50 % mice in the ethanol group. In the control group, one mouse developed a single nodule. All nodules were histologically trabecular HCC composed of eosinophilic and vacuolated cells. In the livers of both control and ethanol group,

several foci with cellular alteration were present, which were significantly higher in ethanol group. Staining for CYP2E1, 4-HNE and c-Myc depicted marked upregulation of all these molecules in the FCA.

**Conclusions** Our data demonstrated that upregulation of CYP2E1 and subsequent production of reactive oxygen species along with the persistent expression of c-Myc play a significant role in the pathogenesis of HCC during chronic ingestion of ethanol.

**Keywords** Hepatocellular carcinoma · HCC · Ethanol · Carcinogenesis · Cellular alteration

## Introduction

Hepatocellular carcinoma (HCC) is the most common type of liver cancer and advanced HCC is always associated with a dismal prognosis [1]. HCC is the third most common cause of cancer-related mortality worldwide and it ranks sixth in terms of global incidence [2]. The major causes of HCC are chronic infection of hepatitis B and C viruses (HBV and HCV) and alcoholic liver cirrhosis [3, 4]. In chronic HBV infection, the integration of the viral DNA into infected cellular machinery can directly induce development of HCC [5]. The persistent infection of HCV and chronic alcoholism will lead to the development of cirrhosis due to perpetual and impaired wound-healing process [6–8]. During this repeated repair and regeneration process, genomic aberrations and mutations could occur, which lead to carcinogenesis [9, 10]. Another major cause for the pathogenesis of HCC is exposure to aflatoxin, a potent liver carcinogen [11]. Furthermore, aging is a risk factor for the development of HCC where the ability of

M. Tsuchishima · J. George (✉) · H. Shiroeda · T. Arisawa ·  
M. Tsutsumi (✉)  
Department of Gastroenterology, Kanazawa Medical University,  
Uchinada, Ishikawa 920-0293, Japan  
e-mail: georgej@kanazawa-med.ac.jp

M. Tsutsumi  
e-mail: tsutsumi@kanazawa-med.ac.jp

T. Takegami  
Medical Research Institute, Kanazawa Medical University,  
Uchinada, Ishikawa 920-0293, Japan

precise DNA repair is depleted, which leads to cellular aberration and carcinogenesis [12].

Even though there are several risk factors for the pathogenesis of HCC, chronic alcohol consumption is considered as one of the major risk factors for hepatocarcinogenesis in humans [13, 14]. Despite the identification of major etiological agents, the molecular mechanisms leading to the development of HCC remains poorly understood and appear to be extremely complex. The upper gastrointestinal tract and liver are the major sites where ethanol-related cancers occur. The mechanism of ethanol-associated carcinogenesis is still obscure [15]. The carcinogenic effects of ethanol could be explained in terms of metabolic modification of pro-carcinogens into more active forms [15, 16]. It is well known that alcohol induces cytochrome P4502E1 (CYP2E1), an enzyme responsible for metabolism of large number of toxins, chemicals, and pro-carcinogens [17, 18]. Conversion of pro-carcinogens into carcinogens occurs through the CYP2E1 mediated drug-metabolizing system present in the microsomes [19]. This induction of CYP2E1 by ethanol could be partly responsible for the high incidence of gastrointestinal and hepatic cancer in chronic alcoholic individuals [20].

Although there are several studies based on the assumption of increased conversion of pro-carcinogens into carcinogens through microsomal CYP2E1, there is no experimental evidence to confirm the pathogenetic correlation between alcohol abuse and development of cancer [15, 21]. An insight of the underlying molecular mechanisms by which chronic alcohol consumption promotes carcinogenesis is important for the development of appropriate strategies for prevention and/or treatment of alcohol-associated cancers. Therefore, in order to understand whether ethanol alone causes HCC and also the mechanisms of ethanol-induced HCC, we fed mice with alcohol for 60 and 70 weeks.

## Materials and Methods

### Animals

All animal experiments were carried out with the *Guide for the Care and Use of Laboratory Animals* published by the US National Institutes of Health (NIH Publication No. 86-23, revised 1996) and also in compliance with Kanazawa Medical University Animal Care and Research Committee. In the present study, we employed ICR (Institute for Cancer Research) mice, which are susceptible to induced carcinogenesis. Besides, there is an average of 85 % similarity between mouse and human genes [22]. The animals were procured from Japan SLC (Hamamatsu, Shizuoka, Japan).

### Treatment of Mice with Ethanol

Approximately 5-week-old ICR male mice weighing 30–35 g were used for the experiment. The animals were maintained in pathogen-free air-conditioned rooms with 12-h light and dark cycles and food available ad libitum. The commercial mice feed was procured from Nosan Corporation, Yokohama, Japan. The composition of the diet fed was carbohydrates 51.4 %, protein 18.7 %, total fat 4.1 %, fiber 5.7 %, essential elements and minerals 4.23 %, amino acids 7.36 %, vitamins 0.31 %, and water 8.2 %, which provides 259.2 kcal for every 100 g. Twenty mice were given water containing 5 % ethanol during the first week, 10 % ethanol during the next 8 weeks, and 15 % ethanol thereafter ad libitum for 60 and 70 weeks. Another set of 20 mice received drinking water without ethanol and served as the control. Five mice were placed per cage on hygienic animal beddings with proper humane care. The drinking water was changed every day and the volume of water consumed was monitored. Animal body weight was recorded on every week. None of the animals died during the entire period of study.

### Examination of Liver Tissue for Tumorigenesis

Ten animals in both groups were killed at weeks 60 and 70 after the start of the study. Blood was collected, allowed to clot for 3–5 h, and serum was separated following the conventional method. Serum alanine transaminase (ALT) and aspartate transaminase (AST) were measured using an auto-analyzer. The livers were carefully removed and weighed, then examined under a stereoscopic microscope and photographed. The liver tissue of every mouse was cut into slices of 5 mm and examined under a stereoscope for the development of nodules and photographed. A portion of the liver was fixed in 10 % phosphate-buffered formalin for histopathological studies. The remaining liver tissue was stored at  $-80^{\circ}\text{C}$  for protein analysis. The paraffin-embedded tissues were cut into sections of 5  $\mu\text{m}$  thickness, heated in a vacuum oven at  $60^{\circ}\text{C}$  for 20 min, deparaffinized with xylene and alcohol, and hydrated. The sections were then stained with hematoxylin and eosin (H&E) for histopathological evaluations. The foci of cellular alteration (FCA) was identified and photographed. The number and size of FCA in the liver tissue was determined using WinRoof image analyzing software (Mitani Co., Fukui, Japan).

### Immunohistochemical Staining for CYP2E1, 4-HNE, and c-Myc

The immunohistochemical staining for CYP2E1, 4-hydroxy-nonenal (4-HNE), and c-Myc was carried out on

paraffin sections. The liver sections were deparaffinized using xylene and alcohol and hydrated to water. Immunohistochemistry was performed using a broad-spectrum histostain kit (Invitrogen, Carlsbad, CA, USA). After blocking, the liver sections were treated with CYP2E1, c-Myc (Abcam, Cambridge, MA, USA) and 4-HNE (Nikken Seil Co., Shizuoka, Japan) primary antibodies and incubated in a moisturized slide chamber (Evergreen Scientific, Los Angeles, CA, USA) at 4 °C for overnight. The antibodies were diluted as per the manufacturer's instructions. The sections were then washed three times in cold PBS and incubated with broad-spectrum biotinylated secondary antibody for 2 h at room temperature. The slides were washed again and treated with streptavidin-peroxidase conjugate and incubated for another 1 h at RT. The final stain was developed using 3 % 3-amino-9-ethylcarbazole (AEC) in *N,N*-dimethylformamide. The stained sections were washed and counterstained with Mayer's hematoxylin for 1 min and mounted using aqueous-based mounting medium. The slides were examined under a microscope (Olympus BX50, Tokyo, Japan) attached with a digital camera (Olympus DP71) and photographed. The staining intensity in ten randomly selected microscopic fields were quantified using WinRoof image analyzing software (Mitani Co., Fukui, Japan).

### Statistical Analysis

Arithmetic mean and standard deviation (mean  $\pm$  SD) were calculated for the data. The results were statistically evaluated using Student's *t* test or  $\chi^2$  test. A value of  $p < 0.05$  was considered as statistically significant. Pearson and Lee's correlation coefficient was used to evaluate the correlation between staining intensity of CYP2E1 and 4-hydroxyl-nonenal in paraffin liver sections. A value of correlation coefficient,  $r < 0.95$  is considered as significant.

## Results

### Alteration of Animal Body Weight and Liver Weight

The average daily intake of drinking water during the period of experiment was  $1.46 \pm 0.11$  ml/mouse in ethanol group and  $1.65 \pm 0.13$  ml/mouse in the control group. The difference was not statistically significant between the groups. Figure 1a demonstrates an alteration of animal body weight during the entire period of the study. The animal body weight was not altered significantly between ethanol and control groups during the study. Figure 1b represents the animal body weight and

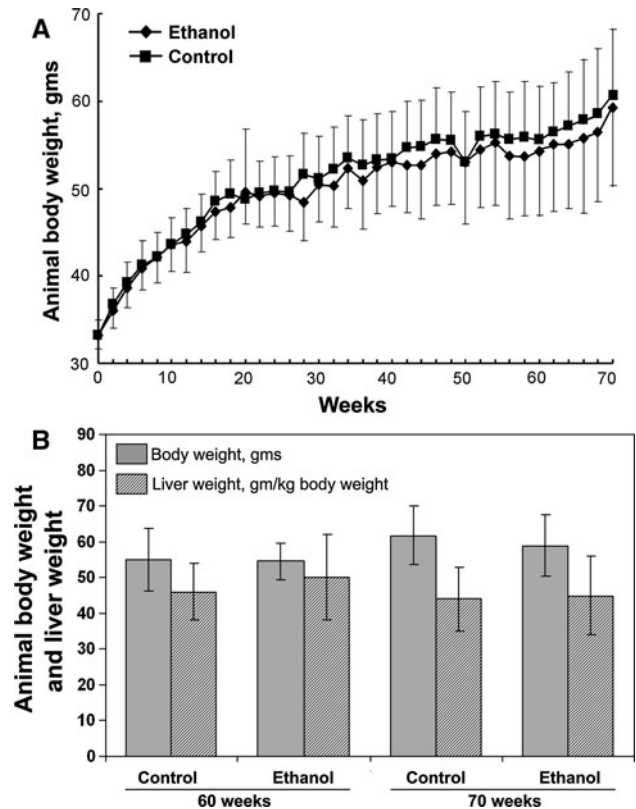


**Fig. 1** a Alteration of body weight in control and ethanol-treated mice during the entire period of study. b Body weight and liver weight at 60 and 70 weeks of the study. Values are mean  $\pm$  SD ( $n = 10$ )

the liver weight normalized to kilogram of body weight at the time of killing. There was no significant difference in body weight and the liver weight normalized to body weight between control and ethanol groups killed both at 60 and 70 weeks. Similarly, there was no significant alteration in serum AST and ALT levels between control and ethanol-treated animals killed at both 60 and 70 weeks.

### Incidence of Hepatic Tumors at 60 and 70 Weeks

At week 60, macroscopic observation revealed four out of the ten mice (40 %) had hepatic white tumors (5–10 mm in diameter) in the ethanol group, while such tumors were completely absent in the control group (Fig. 2a, b; Table 1). At week 70, larger tumors measuring 5–22 mm in diameter developed in the liver in five out of the ten mice (50 %) in the ethanol group (Fig. 2c). In the control group, a single hepatic tumor was developed in one out of the ten mice (10 %). The frequency and size of hepatic tumors in the ethanol

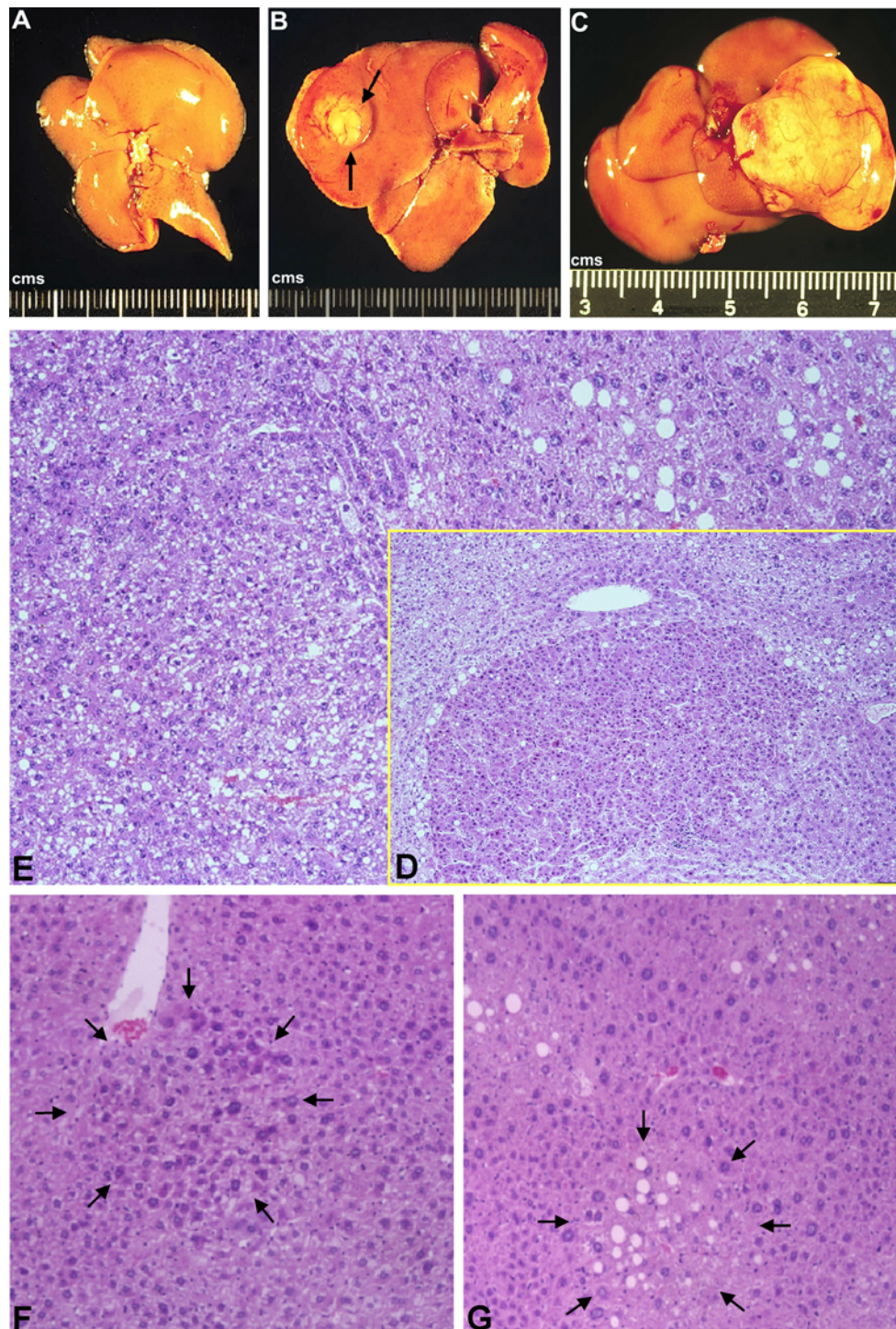


**Fig. 2** a–c Stereoscopic images of the liver tissue of ethanol administered mice at weeks 60 and 70. **a** Control group (60 W): no tumor. **b** Ethanol group (60 W): hepatic tumor was observed. **c** Ethanol group (70 W): large hepatic tumor measuring 22 mm was present. **d–g** H&E staining of liver tissue after administration of

ethanol for 70 weeks. **d** Hepatic tumor depicting invasion and compression of the surrounding tissue ( $\times 100$ ). **e** Higher magnification of hepatic tumor ( $\times 400$ ). Tissue composed of eosinophilic and vacuolated cells. **f** Eosinophilic focus of cellular alternation ( $\times 400$ ). **g** Clear cell focus of cellular alternation ( $\times 400$ )

group was remarkably higher compared to the control group (Table 1). In the ethanol group, the size of hepatic tumors at week 70 ( $12.0 \pm 6.0$  mm in width)

was larger than at week 60 ( $7.5 \pm 1.3$  mm in width) (Table 1). In most cases, there was only a single large hepatic tumor.

**Table 1** The incidence and size of hepatic tumors at 60 and 70 weeks during the study

Groups	Incidence	Size and incidence of the tumor (mm)			
		<5	>5–10<	>10–15<	>15
Control (60 W)	0/10 (0 %)	–	–	–	–
Ethanol (60 W)	4/10 (40 %)**	0	4	0	0
Control (70 W)	1/10 (10 %)	–	1	–	–
Ethanol (70 W)	5/10 (50 %)**	0	3	1	1

\*\*  $p < 0.01$  compared to mean control values

### Histopathology of Alcohol-Induced Hepatic Tumors

The H&E staining of alcohol-induced hepatic tumors at 70 weeks are presented in Fig. 2d–g. The nodules were histologically trabecular HCC, which compressed the surrounding tissue (Fig. 2d). In the trabecular growth of HCC, atypical hepatocytes often exhibited enlarged hyperchromatic nuclei with occasional cluster of clear nucleoli. The tumor cells were composed of eosinophilic and vacuolated cells in addition to numerous small hepatocytes undergoing mitosis (Fig. 2e).

### Foci of Cellular Alteration

We have observed two distinct types of hepatic parenchymal lesions (eosinophilic or clear cell) and identified as FCA in both ethanol and control group mice livers. These lesions were variable in size, ranged from 49 to 150  $\mu\text{m}$  in diameter, and exhibited strong deviation from normal hepatocellular architecture (Figs. 2f, g, 3d, 4d). Portal triads, bile ducts, and macrophage aggregation were generally excluded from these altered foci. Steatosis was present in certain cases. Mitoses were rarely observed. The foci were either eosinophilic (Fig. 2f) or clear cell (Fig. 2g) with a higher frequency of clear cell foci in ethanol-treated animals. In eosinophilic foci, the cytoplasm was eosinophilic with a ground glass or fibrillar nature. In some foci, nuclei were intensely hyperchromatic and pleomorphic. Clear cell foci varied considerably in shape and consisted of extensively vacuolated hepatocytes. The incidence of FCA was 2–3/ hepatic lobule in ethanol group and 1–2/hepatic lobule in control group at 60 and 70 weeks (Table 2). The frequency of FCA was significantly different ( $p < 0.05$ ) between the ethanol and control groups both at 60 and 70 weeks. The size of FCA in the ethanol group was also significantly larger compared to the control group both at weeks 60 and 70 (\* $p < 0.05$  and \*\* $p < 0.01$ , respectively) (Table 2).

### Immunohistochemistry for CYP2E1 in Hepatic Tumors

The immunohistochemical staining for CYP2E1 in the liver tissue after chronic administration of ethanol in the 70-week-old mice is demonstrated through Fig. 3a–f. In control mice, there was moderate staining for CYP2E1 in the pericentral area (Fig. 3a). A similar staining pattern was observed in control mice with hepatic tumor (Fig. 3b). However, the CYP2E1 staining was much less in the tumor area and also localized compared to normal pericentral area (Fig. 3b). There was strong staining for CYP2E1 in the pericentral area of alcohol-treated mice without hepatic tumor compared to age-matched untreated control mice indicating upregulation of CYP2E1 after chronic administration of ethanol (Fig. 3c). Focalized conspicuous staining was present in the mouse liver with precancer zone of FCA indicating dramatic upregulation of CYP2E1 (Fig. 3d). The staining was absent in vacuolated cells in the core of FCA (arrow). There was remarkable staining for CYP2E1 in the area depicting progressive hepatic carcinogenesis (Fig. 3e, arrow). However, CYP2E1 staining was absent in the surrounding areas where tumor cells are already formed (Fig. 3e). Staining for CYP2E1 was very feeble and focalized in well-developed hepatic tumor (Fig. 3f). The staining intensity of CYP2E1 in control and alcohol-treated mice liver was quantified using image analysis software and is represented in Fig. 3g. There was significant increase ( $p < 0.001$ ) in the staining for CYP2E1 in chronic alcohol-treated mice compared to age-matched non-treated control (Fig. 3g). Similarly, there was a significant decrease ( $p < 0.001$ ) in CYP2E1 staining in alcohol-induced hepatic tumor compared to non-treated control mice tumor (Fig. 3g).

### Increase of 4-HNE in Alcohol-Treated Hepatic Tissue

4-hydroxynonenal (4-HNE) is a highly reactive aldehyde generated by the exposure of polyunsaturated fatty acids to peroxides and reactive oxygen species (ROS) and used as a marker for free radicals and oxidative stress. Figure 4a–f depicts the staining for 4-HNE in the liver tissue of 70-week-old mice after chronic administration of ethanol. Staining for 4-HNE was completely absent in control mice (Fig. 4a). Moderate staining was present in the control mice liver with hepatic tumor (Fig. 4b). However, the staining was much less and focalized in the tumor tissue. There was feeble and focalized staining for 4-HNE in alcohol-treated mice without hepatic tumor (Fig. 4c). Conspicuous and highly focalized staining was present in the precancer zone with FCA indicating dramatic increase of 4-HNE (Fig. 4d). The staining for 4-HNE was completely absent in vacuolated cells in the core of FCA

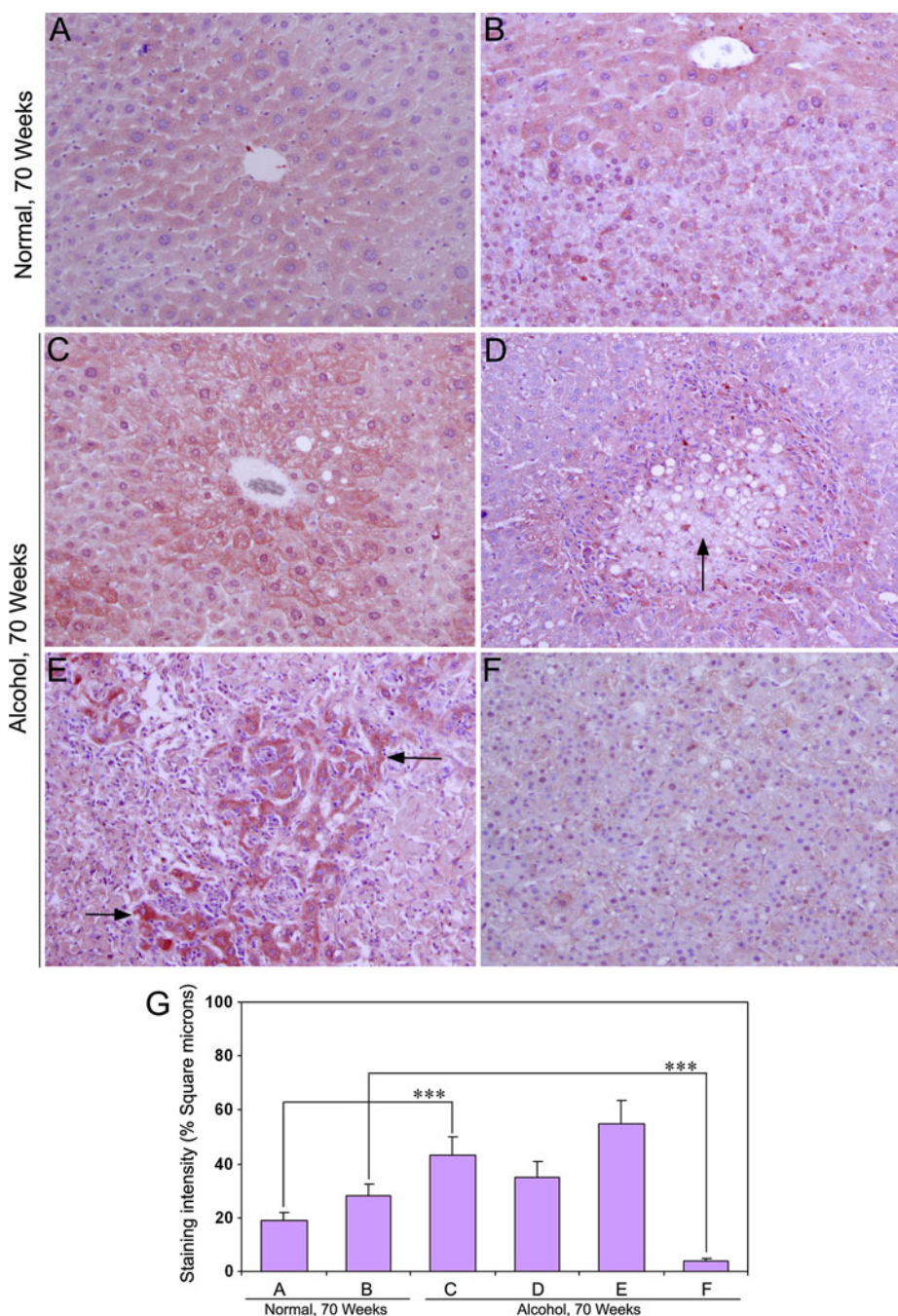


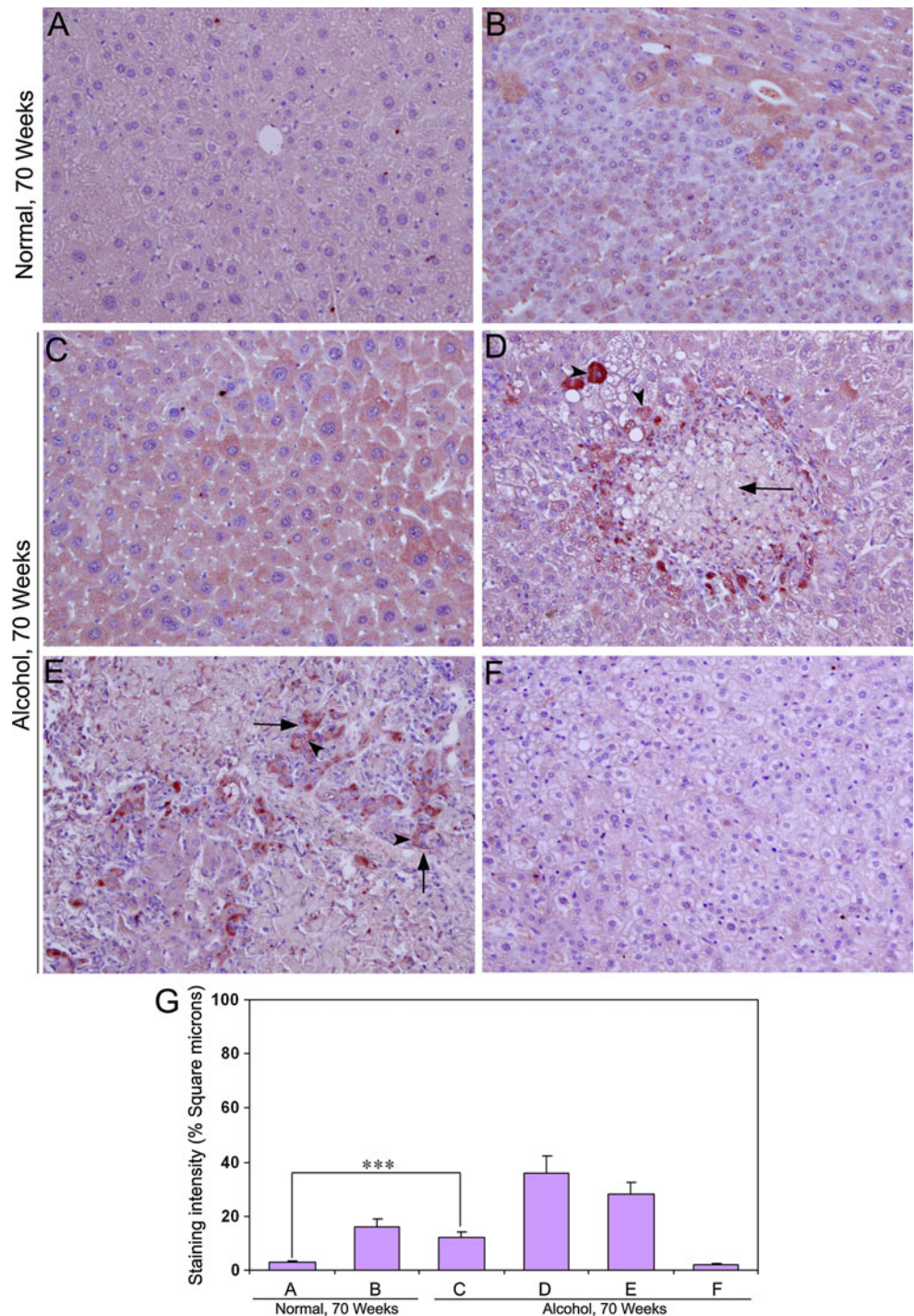
**Fig. 3** Immunohistochemical staining for CYP2E1 in livers of mice administered ethanol for 70 weeks. **a** Control mice ( $\times 100$ ). Moderate staining in pericentral area. **b** Control mice liver with normal area and hepatic tumor ( $\times 100$ ). Moderate staining in pericentral area with normal tissue and focal staining in tumor area. **c** Alcohol-treated mice with normal liver ( $\times 100$ ). Strong staining in pericentral area. **d** Alcohol-treated mice liver depicting normal and precancer foci ( $\times 100$ ). Marked staining of cells surrounding precancer zone

indicating remarkable upregulation of CYP2E1. **e** Alcohol-treated mice liver with normal and tumor area depicting progressive carcinogenesis and conspicuous staining of CYP2E1 in borderline cells ( $\times 100$ ). **f** Mice liver with well developed HCC ( $\times 100$ ). Feeble staining of CYP2E1. **g** Quantitative representation of the staining intensity of CYP2E1 in **a–f** stained sections. The data are mean  $\pm$  SD of six liver samples

(arrow). There was marked staining for 4-HNE in the borderline area with progressive hepatic carcinogenesis (Fig. 4e, arrow) indicating enhanced oxidative stress.

However, the staining was feeble and focalized in the surrounding areas where tumor cells are already formed (Fig. 4e). Staining for 4-HNE was completely absent in

**Fig. 4** Immunohistochemical staining for 4-HNE in livers of mice administered ethanol for 70 weeks. **a** Control mice ( $\times 100$ ). Absence of 4-HNE staining. **b** Control mice liver depicting tumor and normal area ( $\times 100$ ). Absence of staining in tumor area and moderate staining in normal area. **c** Alcohol-treated mice with normal liver ( $\times 100$ ). Moderate staining in pericentral hepatocytes. **d** Alcohol-treated mice liver with normal and precancer area ( $\times 100$ ). Strong staining in cells surrounding precancer zone indicating increased oxidative stress. 4-HNE adduct aggresomes were present in macrophages and hepatocytes (arrowhead). **e** Alcohol-treated mice liver with normal and tumor area depicting progressive carcinogenesis and marked staining in borderline cells ( $\times 100$ ). Presence of 4-HNE adduct aggresomes in hepatocytes (arrowhead). **f** Alcohol-treated mice liver with well-developed HCC ( $\times 100$ ). Complete absence of 4-HNE staining. **g** Quantitative representation of the staining intensity of 4-HNE in **a–f** stained sections. The data are mean  $\pm$  SD of six liver samples



well-formed hepatic tumor tissue (Fig. 4f). We have also observed 4-HNE adduct aggresomes in macrophages and hepatocytes (arrowhead, Fig. 4d, f). The staining intensity of 4-HNE was quantified using image analysis software and presented in Fig. 4g. There was a significant increase ( $p < 0.001$ ) in the staining for 4-HNE in chronic alcohol-treated mice compared to non-treated control (Fig. 4g). Correlation analysis between staining intensity of CYP2E1

and 4-hydroxyl-nonanal in the livers of alcohol-treated animals depicted a significant correlation ( $r = 0.993$ ).

#### Marked Upregulation of c-Myc in Hepatic Tumors

The staining for c-Myc in the liver tissue of 70-week-old mice after chronic administration of ethanol is demonstrated through Fig. 5a–f. Staining for c-Myc was absent in

**Table 2** Size and incidence of focus of cellular alteration in HCC at 60 and 70 weeks

Groups	Incidence/hepatic lobule ( $n = 10$ )	Diameter ( $\mu\text{m}$ )	Size ( $\mu\text{m}^2$ )
Control (60 W)	$1.5 \pm 0.6$	$69.6 \pm 20.1$	$3,800 \pm 1,400$
Ethanol (60 W)	$2.3 \pm 1.2^*$	$83.8 \pm 22.5^*$	$5,500 \pm 1,900^*$
Control (70 W)	$1.8 \pm 0.8$	$70.4 \pm 23.3$	$3,900 \pm 1,700$
Ethanol (70 W)	$2.7 \pm 1.1^{**}$	$88.8 \pm 25.2^{**}$	$6,200 \pm 2,500^{**}$

\*  $p < 0.05$  and \*\*  $p < 0.01$  compared to mean control values

control mice (Fig. 5a). There was moderate staining in the normal liver tissue and strong, but focalized staining in the tumor tissue of control mice with hepatic tumor (Fig. 5b). In alcohol-treated mice without hepatic tumor, the staining for c-Myc was feeble and focalized (Fig. 5c). There was stark staining for c-Myc in the whole area of FCA indicating marked upregulation (Fig. 5d). Focalized strong staining was present in the precancer zone with progressive hepatic carcinogenesis (Fig. 5e). However, the staining was feeble in the surrounding normal tissue. This indicates expression of c-Myc as a marker hepatic tumorigenesis in mice. There was conspicuous and remarkable staining for c-Myc in the whole area of well-developed hepatic tumor demonstrating dramatic upregulation of the molecule in the tumor tissue (Fig. 5f). Quantitative evaluation of c-Myc staining intensity was presented in Fig. 5g. There was a significant increase ( $p < 0.001$ ) in the staining intensity of c-Myc in the normal tissue of chronic alcohol-treated mice compared to age-matched non-treated control (Fig. 5g).

#### Examination for Tumor Induction in Other Organs

In addition to liver, all other major organs such as tongue, esophagus, stomach, colon, pancreas, kidney, and lung were examined both stereoscopically and histopathologically for nodular lesions and focus of cellular alternation in the same manner as in the case of liver tissue at weeks 60 and 70 after chronic administration of ethanol. However, nodular lesions or focus of cellular alternation was absent in all other organs examined.

#### Discussion

Administration of ethanol through drinking water is a very feasible method to study the long-term effect of alcohol on the pathogenesis of HCC. The ICR mouse has been described by Rice and O'Brien [23] and is known for

susceptibility to induced colon cancer. In the present study, ICR mice were fed with ethanol-containing drinking water without any carcinogen or procarcinogen for a period of 60 and 70 weeks to evaluate whether ethanol itself induces pathogenesis of HCC. We have observed well-developed HCC in 40 and 50 % of mice treated with ethanol for 60 and 70 weeks, respectively. On the other hand, HCC was not developed in mice fed with water for 60 weeks and only in 10 % of mice (one out of ten) fed with water for 70 weeks. The incidence of development of HCC in mice treated with ethanol was significantly higher compared to mice fed with water. Our data clearly demonstrate that long-term consumption of ethanol could induce the pathogenesis of HCC.

The present study demonstrates that ethanol induces HCC in mice without the presence of any carcinogen or procarcinogen. Since mouse relish to ingest alcohol compared to other rodents, including rat, mouse is considered as a suitable model to study the long-term effects of ethanol in brain and other organs. In the present study, we observed single large white tumors up to 22 mm in size that were histologically trabecular and resemble human HCC in cellular architecture. Most tumor cells were in mitotic stage and just half in size compared to healthy normal cells, which indicates fast multiplication.

The molecular mechanism of the pathogenesis of alcohol-induced HCC is not clear. Chronic intake of alcohol produces proinflammatory cytokines and chemokines through monocyte activation and increases concentrations of circulating endotoxin [24]. This process activates Kupffer cells, which in turn release many chemokines and cytokines including  $\text{TNF}\alpha$ ,  $\text{IL-1}\beta$  and -6, and causes hepatocyte injury [24]. In perpetual exposures to ethanol, hepatocytes depict increased sensitivity to the cytotoxic effects of  $\text{TNF}\alpha$ , which triggers chronic hepatocyte destruction, stellate cell activation, fibrosis, cirrhosis, and ultimately HCC [25, 26]. The persistent hepatic damage and regeneration during fibrogenesis and formation nodular cirrhosis, genomic aberrations, and mutations could occur, which lead to carcinogenesis [27]. Beland et al. [28] reported that in B6C3F1 mice, alcohol exposure over 104 weeks in drinking water increased HCC, which was significantly dose-related. They reported that the increase in hepatocellular tumors occurred in a relatively linear manner and was attributed to the formation of 1,  $N^6$ -ethenodeoxyadenosine in hepatic DNA coupled with an increase in cell replication.

Alcohol metabolism also impairs the liver through oxidative stress and generation of ROS [29]. Oxidative stress and ROS promote HCC in several ways. Oxidative stress plays a significant role in the pathogenesis of hepatic fibrosis and cirrhosis, which are prominent factors for hepatocarcinogenesis. The pro-carcinogenic effect of the



**Fig. 5** Immunohistochemical staining of c-Myc during pathogenesis of alcohol-induced hepatocellular carcinoma.

**a** Control mice ( $\times 200$ ).

Absence of c-Myc staining.

**b** Control mice liver depicting normal and tumor area ( $\times 100$ ).

Moderate staining in normal area and strong staining in tumor area. **c** Alcohol-treated mice with normal liver ( $\times 100$ ).

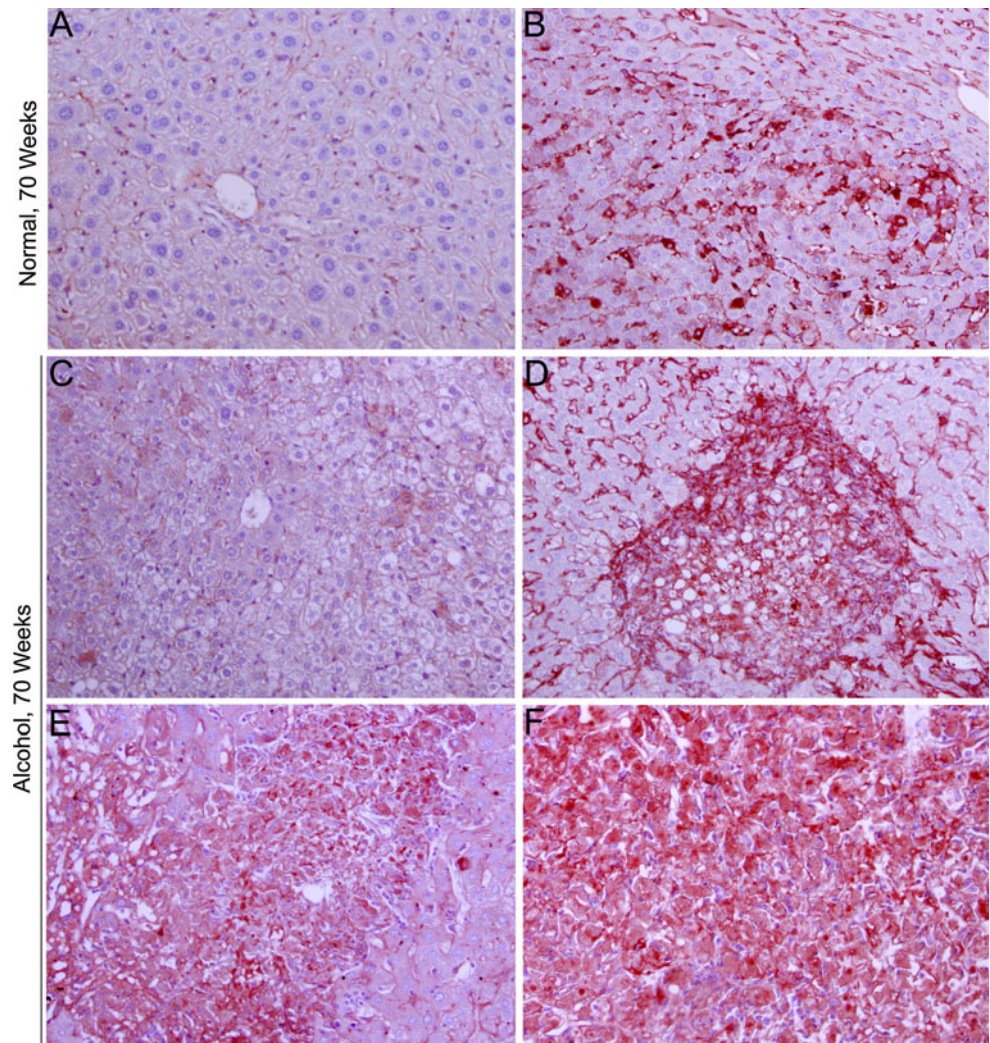
Focalized feeble staining.

**d** Alcohol-treated mice liver depicting normal and precancer area ( $\times 100$ ). Marked staining of c-Myc in the precancer zone indicating dramatic upregulation.

**e** Alcohol-treated mice liver with normal and tumor area demonstrating progressive carcinogenesis with conspicuous staining of c-Myc in tumor borderline areas ( $\times 100$ ).

**f** Alcohol-treated mice liver with well-developed HCC ( $\times 200$ ). Remarkable staining of c-Myc in the entire tumor area.

**g** Quantitative representation of the staining intensity of c-Myc in **a–f** stained sections. The data are mean  $\pm$  SD of six liver samples



cirrhotic microenvironment has been shown in the mouse, where PDGF transgenic mice develop fibrosis that progresses to HCC [30]. Alcohol induces CYP2E1, which contributes to ROS production through the microsomal ethanol oxidizing system (MEOS) [31]. Furthermore, alcohol reduces the levels of potent antioxidants, which scavenge ROS and protects the liver from ROS-induced injury. In the present investigation, we have observed strong induction of CYP2E1 in the pericentral area of livers

of mice treated with alcohol for 70 weeks and also marked upregulation of CYP2E1 in the area of hepatocarcinogenesis (Fig. 3). A similar staining pattern was observed in serial sections in the case of 4-HNE, a marker for oxidative stress and ROS (Fig. 4). In the present study, we have visualized 4-HNE adduct aggregates in both macrophages (Fig. 4d) and hepatocytes (Fig. 4e). The presence of 4-HNE adducts is a characteristic marker of active liver disease [32]. The strong positive correlation ( $r = 0.993$ )

observed between staining intensity of CYP2E1 and 4-HNE in the livers of alcohol-treated animals indicates the role of CYP2E1 in the production of ROS leading to hepatocarcinogenesis.

Ageing is also a risk factor for pathogenesis of HCC, where the cells are more prone to aberration and mutation due to depleted ability of precise DNA repair [12]. The spectrum of hepatocellular hyperplasia in 2-year-old B6C3F1 mice was higher compared to other rodent strains [33]. Since the incidence of hepatocarcinogenesis with aging is low in ICR mice compared with other strains, we used ICR mice in the present investigation. A large study comprising 564 CD-1 (ICR) male mice reported only 3 % of HCC at the age of 105 weeks [34]. Another study involving 300 ICR male mice observed 4.4 % incidence of HCC at 21 months [35]. In another study using B6C3F1 mice, ethanol exposure over 104 weeks in drinking water also increased HCC, which was significantly dose-related [35]. In the present study, we observed spontaneous hepatic tumor only in one mouse out of ten control animals (10 %) at week 70. The percentage of tumor incidence would have been much lower if the number of control animals was notably higher as in previous studies. However, the incidence and size of HCC in ICR mice treated with ethanol was fivefold higher than those of HCC developed with aging, suggesting that chronic alcohol ingestion may promote the development of HCC with aging.

In the present study, we have observed two distinct types of FCA in ethanol treated as well as control mice livers both at 60 and 70 weeks. One or two FCA of preneoplastic lesion per hepatic lobule was found in mice fed with water for 60 weeks. This data suggests the possibility of HCC development if such mice are maintained for longer periods. In mice treated with ethanol, the incidence and size of FCA per hepatic lobule was significantly higher compared to control mice, indicating the effects of ethanol on the formation of precancerous FCA. A similar pattern was observed in the case of FCA in mice treated with ethanol for 70 weeks (Table 2). The clear cell vacuoles present in the FCA are original fat globules or fatty degeneration of hepatocytes (steatosis), which occurred during chronic intake of alcohol. Eventually, the areas with extensive steatosis transform into FCA and may trigger tumorigenesis. In due course, the fat within the globules disappears and the clear vesicles persist. These results suggest that chronic intake of alcohol produces extensive steatosis and accelerates the formation of preneoplastic lesions that lead to HCC.

In an attempt to elucidate the molecular mechanism of the pathogenesis of HCC after chronic administration of ethanol in ICR mice, we stained liver sections for c-Myc. The results showed a conspicuous and dramatic upregulation of c-Myc in both precancerous and well-developed hepatic tumors. The transcription factor c-Myc is considered

as a proto-oncogene and is mutated in many cancers, which cause its persistent expression. The marked upregulation of c-Myc in HCC could cause unregulated expression of many genes involved in anti-apoptosis and cell proliferation, which results in tumorigenesis. The chronic intake of alcohol leads to induction of CYP2E1, which in turn produces oxidative stress and ROS. The highly ROS could generate mutations in the c-Myc gene leading to its persistent expression and dramatic upregulation of c-Myc protein levels as observed in the present study.

In conclusion, our study demonstrated that chronic administration of ethanol through drinking water induces HCC development in ICR mice both at 60 and 70 weeks. Metabolic detoxification of alcohol in the liver induces CYP2E1 and MEOS, which in turn generates oxidative stress and produces ROS. In addition to acetaldehyde, one of the metabolic products of alcohol, the highly ROS injures hepatocytes, which not only triggers several signaling pathways but also accelerates aging of the liver. The toxic and chronic liver injury and the subsequent repeated regeneration process could produce mutations in proto-oncogenes and/or onco-suppressor genes leading to cellular aberration and tumorigenesis. However, further studies are necessary to elucidate the exact molecular mechanism of the pathogenesis of HCC during chronic ingestion of ethanol.

**Acknowledgments** This work was supported by a grant for specially promoted research from Kanazawa Medical University, Japan (SR 2012-04).

**Conflict of interest** None.

## References

1. Chun JM, Kwon HJ, Sohn J, et al. Prognostic factors after early recurrence in patients who underwent curative resection for hepatocellular carcinoma. *J Surg Oncol*. 2011;103:148–151.
2. Parkin DM, Bray F, Ferlay J, Pisani P. Global cancer statistics, 2002. *CA Cancer J Clin*. 2005;55:74–108.
3. Cornellà H, Alsinet C, Villanueva A. Molecular pathogenesis of hepatocellular carcinoma. *Alcohol Clin Exp Res*. 2011;35:821–825.
4. French SW, Oliva J, French BA, Li J, Bardag-Gorce F. Alcohol, nutrition and liver cancer: role of Toll-like receptor signaling. *World J Gastroenterol*. 2010;16:1344–1348.
5. Chemin I, Zoulim F. Hepatitis B virus-induced hepatocellular carcinoma. *Cancer Lett*. 2009;286:52–59.
6. Vezali E, Aghemo A, Colombo M. A review of the treatment of chronic hepatitis C virus infection in cirrhosis. *Clin Ther*. 2010;32:2117–2138.
7. Rehm J, Taylor B, Mohapatra S, et al. Alcohol as a risk factor for liver cirrhosis: a systematic review and meta-analysis. *Drug Alcohol Rev*. 2010;29:437–445.
8. Lefton HB, Rosa A, Cohen M. Diagnosis and epidemiology of cirrhosis. *Med Clin N Am*. 2009;93:787–799.
9. Thorgeirsson SS, Grisham JW. Molecular pathogenesis of human hepatocellular carcinoma. *Nat Genet*. 2002;31:339–346.

10. Wong N, Lai P, Pang E, et al. Genomic aberrations in human hepatocellular carcinomas of differing etiologies. *Clin Cancer Res.* 2000;6:4000–4009.
11. Wogan GN. Aflatoxins as risk factors for hepatocellular carcinoma in humans. *Cancer Res.* 1992;52:2114s–2118s.
12. Montalto G, Cervello M, Giannitrapani L, Dantona F, Terranova A, Castagnetta LA. Epidemiology, risk factors, and natural history of hepatocellular carcinoma. *Ann N Y Acad Sci.* 2002;963:13–20.
13. Pan H, Fu X, Huang W. Molecular mechanism of liver cancer. *Anticancer Agents Med Chem.* 2011;11:493–499.
14. Moradpour D, Blum HE. Pathogenesis of hepatocellular carcinoma. *Eur J Gastroenterol Hepatol.* 2005;17:477–4783.
15. Pöschl G, Seitz HK. Alcohol and cancer. *Alcohol Alcohol.* 2004;39:155–165.
16. Seitz HK, Stickel F. Molecular mechanisms of alcohol-mediated carcinogenesis. *Nat Rev Cancer.* 2007;7:599–612.
17. Wang Y, Millonig G, Nair J, et al. Ethanol-induced cytochrome P4502E1 causes carcinogenic etheno-DNA lesions in alcoholic liver disease. *Hepatology.* 2009;50:453–461.
18. Quertemont E. Genetic polymorphism in ethanol metabolism: acetaldehyde contribution to alcohol abuse and alcoholism. *Mol Psychiatry.* 2004;9:570–581.
19. Tsutsumi M, George J, Ishizawa K, Fukumura A, Takase S. Effect of chronic dietary ethanol in the promotion of *N*-nitrosomethylbenzylamine-induced esophageal carcinogenesis in rats. *J Gastroenterol Hepatol.* 2006;21:805–813.
20. Lieber CS, Garro A, Leo MA, Mak KM, Worner T. Alcohol and cancer. *Hepatology.* 1986;6:1005–1019.
21. Anttila S, Raunio H, Hakkola J. Cytochrome p450-mediated pulmonary metabolism of carcinogens: regulation and cross-talk in lung carcinogenesis. *Am J Respir Cell Mol Biol.* 2011;44:583–590.
22. Su AI, Cooke MP, Ching KA, et al. Large-scale analysis of the human and mouse transcriptomes. *Proc Natl Acad Sci USA.* 2002;99:4465–4470.
23. Rice MC, O'Brien SJ. Genetic variance of laboratory outbred Swiss mice. *Nature.* 1980;283:157–161.
24. McClain CJ, Hill DB, Song Z, Deaciuc I, Barve S. Monocyte activation in alcoholic liver disease. *Alcohol.* 2002;27:53–561.
25. Fattovich G, Stroffolini T, Zagni I, Donato F. Hepatocellular carcinoma in cirrhosis: incidence and risk factors. *Gastroenterology.* 2004;127:S35–S50.
26. Miller AM, Horiguchi N, Jeong WI, Radaeva S, Gao B. Molecular mechanisms of alcoholic liver disease: innate immunity and cytokines. *Alcohol Clin Exp Res.* 2011;35:787–793.
27. Yam JW, Wong CM, Ng IO. Molecular and functional genetics of hepatocellular carcinoma. *Front Biosci (Schol Ed).* 2010;2:117–134.
28. Beland FA, Benson RW, Mellick PW, et al. Effect of ethanol on the tumorigenicity of urethane (ethyl carbamate) in B6C3F1 mice. *Food Chem Toxicol.* 2005;43:1–19.
29. Wu D, Cederbaum AI. Oxidative stress and alcoholic liver disease. *Semin Liver Dis.* 2009;29:141–154.
30. Campbell JS, Hughes SD, Gilbertson DG, et al. Platelet-derived growth factor C induces liver fibrosis, steatosis, and hepatocellular carcinoma. *Proc Natl Acad Sci USA.* 2005;102:3389–3394.
31. Cederbaum AI, Lu Y, Wu D. Role of oxidative stress in alcohol-induced liver injury. *Arch Toxicol.* 2009;83:519–548.
32. Amidi F, French BA, Chung D, Halsted CH, Medici V, French SW. M-30 and 4HNE are sequestered in different aggresomes in the same hepatocytes. *Exp Mol Pathol.* 2007;83:296–300.
33. Maronpot RR, Haseman JK, Boorman GA, Eustis SE, Rao GN, Huff JE. Liver lesions in B6C3F1 mice: the national toxicology program, experience and position. *Arch Toxicol Suppl.* 1987;10:10–26.
34. Baldrick P, Reeve L. Carcinogenicity evaluation: comparison of tumor data from dual control groups in the CD-1 mouse. *Toxicol Pathol.* 2007;35:562–569.
35. Engelhardt JA, Gries CL, Long GG. Incidence of spontaneous neoplastic and nonneoplastic lesions in Charles River CD-1 mice varies with breeding origin. *Toxicol Pathol.* 1993;21:538–541.